NANO LETTERS

Letter

Vertically Aligned p-Type Single-Crystalline GaN Nanorod Arrays on n-Type Si for Heterojunction Photovoltaic Cells

Y. B. Tang, Z. H. Chen, H. S. Song, C. S. Lee, H. T. Cong, H. M. Cheng, W. J. Zhang, I. Bello, and S. T. Lee

Nano Lett., **2008**, 8 (12), 4191-4195 • DOI: 10.1021/nl801728d • Publication Date (Web): 29 October 2008

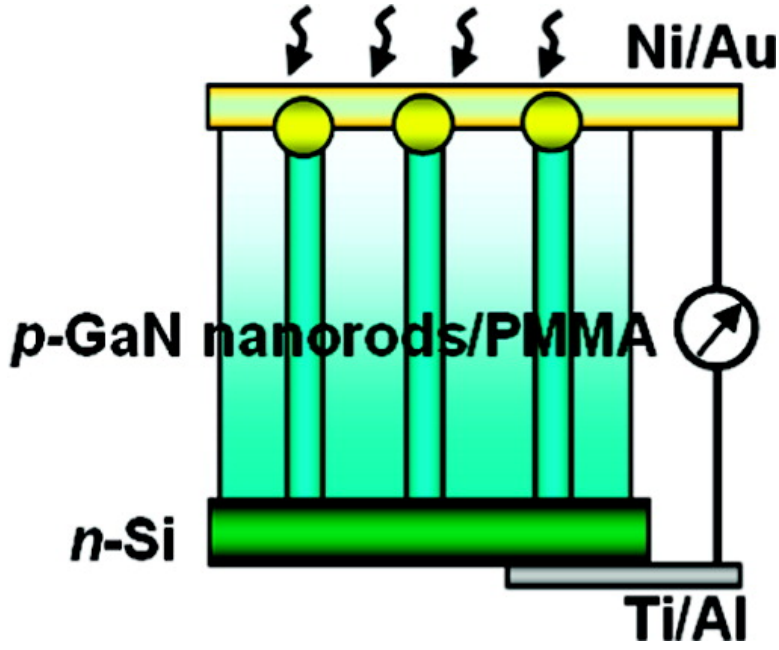

More About This Article

Additional resources and features associated with this article are available within the HTML version:

- Supporting Information
- Access to high resolution figures
- Links to articles and content related to this article
- Copyright permission to reproduce figures and/or text from this article

View the Full Text HTML

NANO LETTERS

2008
Vol. 8, No. 12
4191-4195

Vertically Aligned p-Type Single-Crystalline GaN Nanorod Arrays on n-Type Si for Heterojunction Photovoltaic Cells

Y. B. Tang,[†] Z. H. Chen,[†] H. S. Song,[†] C. S. Lee,*[,†] H. T. Cong,[‡] H. M. Cheng,[‡] W. J. Zhang,[†] I. Bello,[†] and S. T. Lee*[,†]

Center of Super-Diamond and Advanced Films (COSDAF) and Department of Physics and Materials Science, City University of Hong Kong, Hong Kong SAR, People's Republic of China, and Shenyang National Laboratory for Materials Science, Institute of Metal Research, Chinese Academy of Sciences, Shenyang 110016, People's Republic of China

Received June 17, 2008; Revised Manuscript Received September 2, 2008

ABSTRACT

Vertically aligned Mg-doped GaN nanorods have been epitaxially grown on n-type Si substrate to form a heterostructure for fabricating p−n heterojunction photovoltaic cells. The p-type GaN nanorod/n-Si heterojunction cell shows a well-defined rectifying behavior with a rectification ratio larger than 10^4 in dark. The cell has a high short-circuit photocurrent density of 7.6 mA/cm^2 and energy conversion efficiency of 2.73% under AM 1.5G illumination at 100 mW/cm^2. Moreover, the nanorod array may be used as an antireflection coating for solar cell applications to effectively reduce light loss due to reflection. This study provides an experimental demonstration for integrating one-dimensional nanostructure arrays with the substrate to directly fabricate heterojunction photovoltaic cells.

Aligned one-dimensional (1D) nanostructure arrays are potential building blocks for optoelectronic devices, such as nanolasers,[1−3] field-effect transistors,[4] light-emitting diodes,[5−7] diodes,[8] electric generators,[9,10] field emitters,[11,12] and so on. Compared to polycrystalline films, such arrays are particularly advantageous for photovoltaic (PV) application because the oriented geometry provides direct conduction paths for photogenerated carriers to transport from the junction to the external electrode, thereby resulting in a high carrier collection efficiency.[13−15] Several studies have revealed that the carrier diffusion coefficient and electron recombination time of ordered 1D nanostructures are much larger than those for polycrystalline films, which may remarkably increase the diffusion length of minority carrier.[16−19] It has been reported that electron transport in crystalline wires is several orders of magnitude faster than that in the polycrystalline counterpart and leads to a lower recombination loss and a higher photocurrent.[20−22] Moreover, on comparison with thin films, 1D nanostructure arrays typically have low optical reflectance over a wide spectral range.[23−25] Photovoltaic properties of various 1D nanostructure arrays such as TiO_2 nanotubes,[16−18,26,27] ZnO nanotubes,[13−15,19,28] and Si[23,29] nanowires have been investigated, and they indeed showed superior performance over their film and bulk counterparts.

Gallium nitride (GaN) 1D nanostructure arrays of high crystalline quality are attractive for high-performance nanodevices due to the merits of GaN including a wide and direct band gap, high carrier mobility, high thermal and chemical stability, and capability of n- or p-type doping.[30,31] Compared to thin films, heterostructures on GaN 1D nanostructure arrays with low defect density are much easier to fabricate and lead to high-performance devices.[8] So far, arrays of GaN 1D nanostructures have been grown on Si,[32,33] sapphire,[5,34−36] GaN,[8,37,38] $LiAlO_2$, and MgO substrates.[39] Among them, vertically aligned GaN 1D nanostructure arrays on Si substrates may be promising structures for PV applications because both the oriented morphology and a reasonably large band gap difference between the substrate and the GaN 1D nanostructures are readily achieved in these heterostructures. Single-crystalline GaN nanorod arrays on the top of the heterostructure can act as a wide band gap "window" for suppressing the minority-carrier recombination and enhance

* Corresponding authors, apcslee@cityu.edu.hk and apannale@cityu.edu.hk.
[†] Center of Super-Diamond and Advanced Films (COSDAF) and Department of Physics and Materials Science, City University of Hong Kong.
[‡] Shenyang National Laboratory for Materials Science, Institute of Metal Research, Chinese Academy of Sciences.

10.1021/nl801728d CCC: $40.75
Published on Web 10/29/2008

short-wavelength spectral response. In addition, the array of GaN 1D nanostructures can serve as an antireflection layer to reduce the visible optical loss. Although considerable efforts have been devoted to the implementation of GaN 1D nanostructures into nanoscale electronic and photonic devices,[5,8,34,35,40−45] few results in PV cell based on GaN 1D nanostructure arrays are reported. Here, we report on the fabrication of a p-GaN nanorod array/n-Si solar cell and its PV performances. The approach reported here provides a new dimension to the utilization of 1D nanostructure arrays for PV cell applications.

Vertically aligned Mg-doped GaN nanorod arrays on n-type Si substrates were synthesized by a chemical vapor deposition method using gold nanoparticles as catalyst. The growth procedures are described briefly as follows: n-type Si(111) substrates (1 × 2 cm) were first cleaned by a piranha solution (3:1 H_2SO_4:30% H_2O_2) and then immersed into a 5% solution of (3-aminopropyl)trimethoxysilane (APTMS, Aldrich) in ethanol, followed by drying at 90 °C. Afterward, a gold-nanoparticle-seeded Si substrate was prepared by directly bubbling nitrogen through a suspension of negatively charged Au nanoparticle to the substrate vertically placed on the downstream of a horizontal chemical vapor deposition furnace. Upon encountering the aerosolized Au nanoparticles, the amine-functionalized Si substrate surface was partially protonated. Upon electrostatic interaction with the negatively charged nanoparticles,[46] an Au nanoparticle monolayer was formed. Mg-doped GaN nanorod arrays were synthesized by thermal evaporation of a powder mixture of $GaCl_3$ and $MgCl_2$ (30:1 in molar ratio) at 850 °C for 1 h onto the Si substrate which was placed at lower temperature zone of 750−700 °C along the downstream of the gas flow. High-purity ammonia premixed with 5% hydrogen was fed at a total flow rate of 100 sccm.

Morphologies of the GaN nanorod arrays were examined with a field-emission scanning electron microscope (SEM). Figure 1a is a typical SEM image of an as-synthesized GaN nanorod array, which reveals the uniform alignment of GaN nanorods on the substrate. The diameter of these nanorods has a uniform size distribution around 100 nm. A cross-section SEM image (inset, Figure 1a) shows the nanorods grow vertically from the Si(111) substrate with lengths of ∼1.0 μm. The density of the nanorod array is ∼1.0 × 10^9/cm^2. X-ray diffraction (XRD) measurements (not shown here) identified that the GaN nanorods have a hexagonal wurtzite structure. Only diffraction peaks from (0002) and (0004) crystal planes of wurtzite GaN were observed in the XRD spectrum, indicating preferential growth of the nanorods along the [0001] direction. This is further confirmed by transmission electron microscopy (TEM) characterization. Low-magnification TEM images show that each nanorod terminates with a gold nanoparticle, suggesting the catalyst-induced vapor−liquid−solid mechanism of the growth process. High-resolution TEM images and the corresponding selected-area electron diffraction patterns (e.g., Figure 1b and its inset) confirm that the nanorods are single-crystal wurtzite GaN growing along the [0001] orientation. The GaN nanorods are highly crystalline with no observable defects

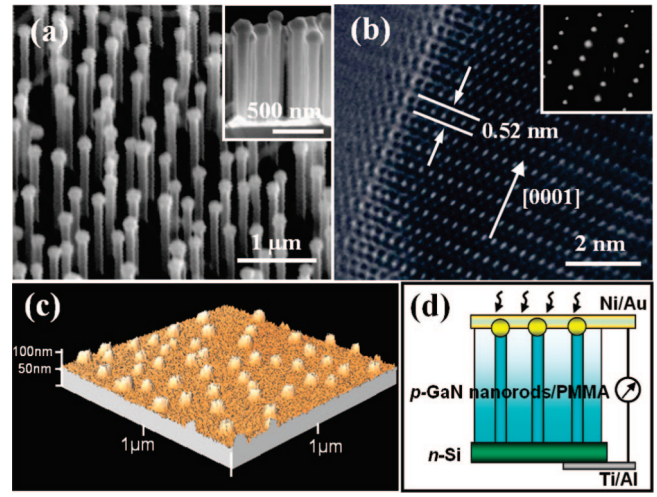

Figure 1. (a) Tilt top view SEM image of Mg-doped GaN nanorod arrays. Inset shows cross-sectional SEM image. (b) HRTEM image of GaN nanorod and its corresponding SAED pattern (inset). (c) AFM image of GaN nanorod tips exposed above the photoresist layer. (d) A schematic of the p-GaN nanorod/n-Si heterojunction photovoltaic cell.

or amorphous shell, as often found in other nanorods. Energy-dispersive X-ray spectroscopy (not shown here) analyses revealed that the Mg element distributed uniformly in the nanorods ranging from 1.1 to 2.4 atom % in different rods.[46]

To demonstrate the viability of the GaN nanorod array for use in PV application, a solar cell (SC) was fabricated. For preparing the heterojunction SC, the spaces between the GaN nanorods were filled with insulating photoresist (PMMA) via spin coating. After photoresist deposition, the surface of the sample was partially dissolved by acetone until the tips of GaN nanorods were exposed for metal contact. Figure 1c presents an atomic force microscopy (AFM) image of the structure with the exposed GaN nanorod tips. Conventional Ohmic contacts were achieved by electron-beam evaporating Ni/Au (30/50 nm) and Ti/Al (30/50 nm) electrodes onto the p-type GaN nanorods and the backside of n-type Si substrate, respectively. A schematic structure of the p-GaN nanorod/n-Si heterojunction SC with an active cell area of 0.5 × 0.5 cm^2 is illustrated in Figure 1d.

Figure 2a shows the current density−voltage ($J-V$) characteristics of the SC measured in dark and under air mass 1.5 global (AM1.5G) illumination from a calibrated solar simulator with an intensity of 100 mW/cm^2 (equivalent to 1 sun). The fabricated heterojunction cell exhibits a clear diode behavior in darkness. Under forward bias, an obvious turn on of the device was observed at ∼1.0 V. At +0.5 V bias, the forward current density of the device was 0.28 mA/cm^2 while the reverse leakage current density was less than 1.8 × 10^{-5} mA/cm^2 at −0.5 V, so the rectification ratio is greater than 10^4 at ±0.5 V, implying a good p−n junction between the p-type GaN nanorod and n-type Si substrate.

Upon illumination of the front surface with simulated sunlight, the device yields an obvious photocurrent. A short-circuit current density J_{SC} of ∼7.6 mA/cm^2 and an open-circuit voltage V_{OC} of ∼0.95 V were obtained under 1 sun

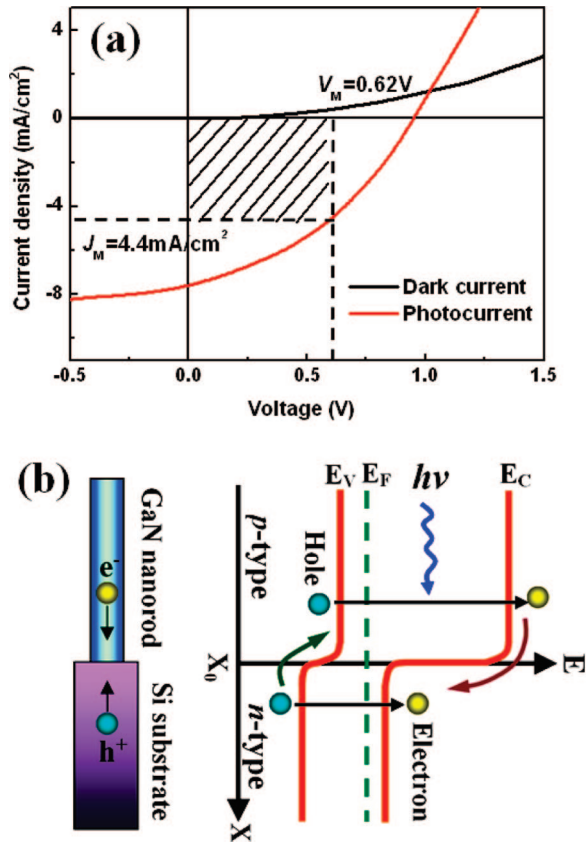

Figure 2. (a) Current density vs voltage for the solar cell in the dark and under simulated AM1.5G illumination with an intensity of 100 mW/cm^2. (b) Schematic energy band diagram of the heterojunction diode showing the photogenerated carrier transfer process.

intensity. Fill factor (FF) and power conversion efficiency (η) were calculated according to the following equations

$$\mathrm{FF} = V_M J_M / V_{OC} J_{SC} \quad (1)$$

$$\eta_{AM1.5} = V_{OC} J_{SC} (\mathrm{FF}) \quad (2)$$

where V_{OC} and J_{SC} are the open-circuit voltage and short-circuit current and V_M and J_M are the voltage and current density at the maximum power output (indicated as the shadowed rectangle in Figure 2a), respectively. From the $J-V$ curve under simulated AM1.5G condition, the FF and η were calculated to be ~0.38 and ~2.73%, respectively. In addition, the photocurrent was obviously higher than the dark current in the first quadrant. Such difference can be attributed to the photoenhanced current.

The rectifying behavior in the dark and the photocurrent phenomenon under illumination of the p-GaN nanorod/n-Si heterojunction cell can be explained by the energy band structure of this heterostructure. Figure 2b shows the schematic energy band diagram of the heterojunction diode at thermal equilibrium. Since the band gaps (E_g) of Si and GaN are 1.1 and 3.4 eV, respectively, an asymmetrical energy barrier would be formed at the junction interface, which leads to a large energy barrier for electrons so that electrons diffusion and recombination with holes in the GaN nanorods become more difficult as a result. The hole injection into the n-type Si side is naturally low due to the built-in field. Therefore, the GaN nanorod array on the top of the heterojunction was used as a wide band gap semiconductor to decrease the leakage current in the depletion region.

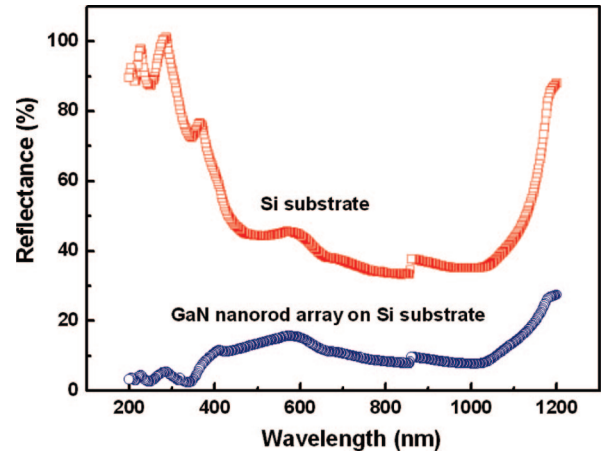

Figure 3. Reflectance measurements of the GaN nanorod array on Si substrate and the bare Si substrate.

When the device is illuminated by the simulated sunlight from the top of p-type GaN nanorods, photons with energy less than E_g (GaN) but greater than E_g (Si) will transmit through the nanorods, acting as an optical "window", and be absorbed by the n-type Si. Part of the light can directly reach the junction via the space between the GaN nanorods. Simultaneously, light with photon energies larger than E_g (GaN) will be absorbed by the GaN nanorods. The holes and electrons generated in both sides of the heterojunction are collected effectively due to the large built-in electric field at the junction and thus yield the photocurrent as schematically shown in Figure 2b. Note that this qualitative analysis neglects the effects of band offset at the junction and the influence of the metal electrodes (expected to be Ohmic contact[5,8,35]). Further work is needed to quantitatively understand the interface of this heterojunction. The single-crystal nature and aligned morphology of the GaN nanorods allow a fast and direct conduction of the photogenerated carriers from the heterojunction to the external electrode, which greatly reduces the recombination losses of the photogenerated carriers and results in a high photocurrent.[17−19] In addition, heavy Mg doping can remarkably lower the series resistance of GaN nanorods and thus increase the charge transport efficiency.

1D nanostructure arrays are shown to serve effectively as an antireflection coating to reduce optical reflection.[23−25] The reduction of optical loss is one important factor for obtaining high-efficiency solar cells. To achieve this goal, the top surface of the solar cells is generally texturized or covered with an antireflection coating (ARC).[47,48] Therefore, the reflectance behavior of the GaN nanorod array was investigated for its potential application as an antireflection layer. Figure 3 shows the reflectance spectra of the as-synthesized GaN nanorod arrays on Si substrate and the bare Si substrate. The reflectivity of a bare Si surface is about 50.4% over the range of 300−700 nm consistent with previous results,[23] while an average of 10.1% reflectance was obtained over the same spectral range for the GaN nanorod array grown on Si substrate, revealing that GaN nanorod array can

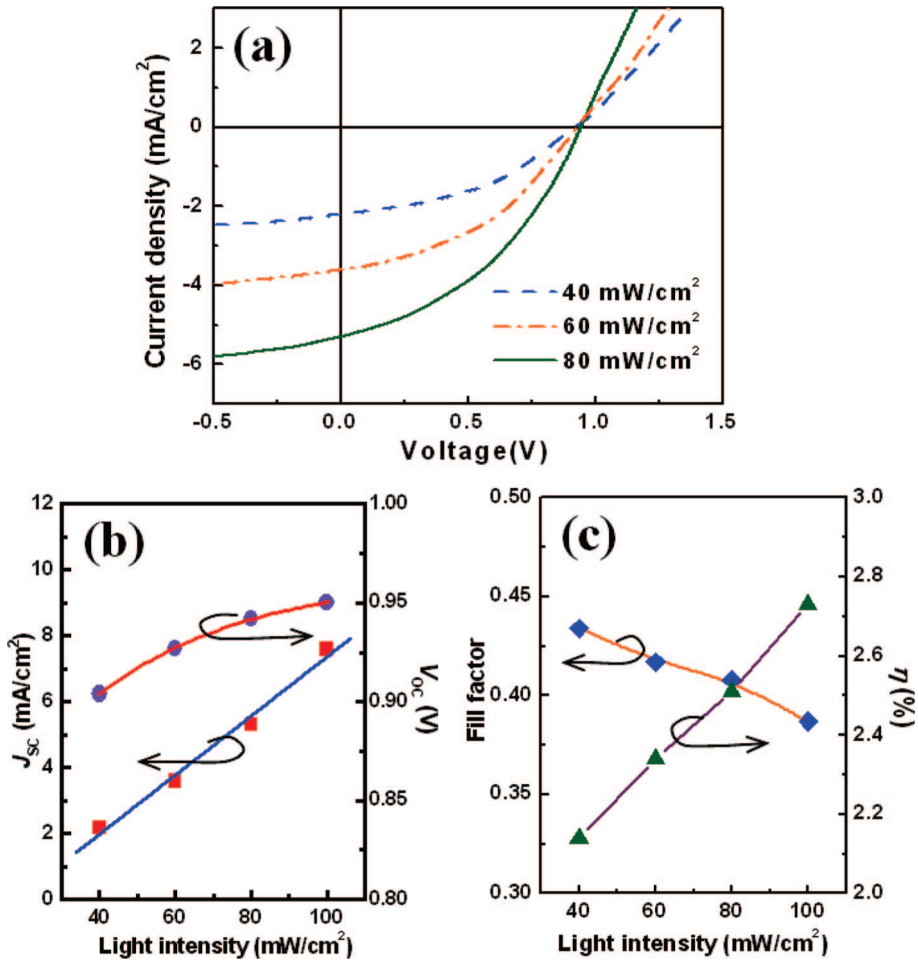

Figure 4. Cell performance under different illumination intensities. (a) $J-V$ curves. (b, c) Short-circuit current density (J_{SC}), open-circuit voltage (V_{OC}), fill factor (FF), and power-conversion efficiency (η) of the cell as functions of light intensity.

effectively act as antireflection coating to decrease reflection, especially in the short wavelength range of 200−400 nm. Low reflectance of the GaN nanorod array originated from its high surface area and nanoscale subwavelength size.[21−23,49,50]

The effect of light intensity on the solar cell performance was also investigated. Figure 4 shows the $J-V$ curves and the variation of the PV performance characteristics under different illumination intensities. The J_{SC} follows an approximately linear relationship with illumination intensity as expected, whereas the V_{OC} shows some increase and then saturates at higher intensity (Figure 4b). On the other hand, FF decreased from 0.43 to 0.38 as the intensity was increased from 40 to 100 mW/cm^2, which is probably due to the increasing resistive loss.[51] Even without full optimization of fabrication process, the energy conversion efficiency of our cell was measured to be >2.0% under all tested illumination intensities (Figure 4c). Note that the Ni/Au metal film contact on top of the nanorod array has a relatively large thickness, which is proved to transmit only about half of the light in the simulated solar spectrum (Figure S1, Supporting Information). Therefore, reducing the thickness of the top metal contact is expected to lead to a higher efficiency.

In summary, a uniform array of Mg-doped GaN nanorods with vertical alignment was grown on n-type Si(111) substrate. The nanorods are single-crystalline and grow along the [0001] direction. Measurements showed that the GaN nanorod array can effectively act as an antireflection coating to reduce the reflection of the visible light. A heterojunction solar cell was directly fabricated from the p-GaN nanorod grown on n-Si, and the cell exhibited well-defined rectifying behavior in the dark with a rectification ratio greater than 10^4 at ±0.5 V. A maximum power conversion efficiency (PCE) of ~2.73% was achieved under 1 sun simulated AM1.5 solar illumination with a high open-circuit voltage of ~0.95 V, a short-circuit current density of ~7.6 mA/cm^2, and a fill factor of ~0.38. The PCE increased with increasing light intensity and could be improved via straightforward optimization such as reducing electrode thickness. This study demonstrated the excellent potential of GaN 1D nanostructure arrays for use in heterojunction PV cells. Significantly, the aligned GaN nanorods can be directly incorporated into the device structure without a complicated fabrication process.

Acknowledgment. The authors thank Drs. Y. Q. Qiao, Y. M. Chong, and S. L. Lai for their kind help with reflectance, AFM, and photovoltaic experiments. The work was supported by a NSFC/RGC Joint Research Scheme (No. N_CityU 125/05) of Research Grants Council of Hong Kong SAR, China, the US Army International Technology Center

- Pacific, and the National 973 projects of the Major State Research Development Program of China (Grant No. 2006CB933000 and Grant No. 2007CB936000).

Supporting Information Available: Photo and SEM images, and optical transmittance spectrum of the glass coated with Ni /Au (30/50 nm) film. This material is available free of charge via the Internet at http://pubs.acs.org.

References

(1) Huang, M. H.; Mao, S.; Feick, H.; Yan, H.; Wu, Y.; Kind, H.; Webber, E.; Russo, R.; Yang, P. *Science* **2001**, *292*, 1897.
(2) Yang, P.; Yan, H.; Mao, S.; Russo, R.; Johnson, J.; Saykally, R.; Morris, N.; Pham, J.; He, R.; Choi, H. J. *Adv. Funct. Mater.* **2002**, *12*, 323.
(3) Jiang, Y.; Zhang, W. J.; Jie, J. S.; Meng, X. M.; Zapien, J. A.; Lee, S. T. *Adv. Mater.* **2006**, *18*, 1527.
(4) Ng, H.; Han, J.; Yamada, T.; Nguyen, P.; Chen, Y. P.; Meyyappan, M. *Nano Lett.* **2004**, *4*, 1247.
(5) Kim, H. M.; Cho, Y. H.; Lee, H.; Kim, S., II; Ryu, S. R.; Kim, D. Y.; Kang, T. W.; Chung, K. S. *Nano Lett.* **2004**, *4*, 1059.
(6) Wang, X. D.; Summers, C. J.; Wang, Z. L. *Nano Lett.* **2004**, *4*, 423.
(7) Park, W. I.; Yi, G. C. *Adv. Mater.* **2004**, *16*, 87.
(8) Deb, P.; Kim, H.; Qin, Y.; Lahiji, R.; Oliver, M.; Reifenberger, R.; Sands, T. *Nano Lett.* **2006**, *6*, 2893.
(9) Wang, Z. L. *MRS Bull.* **2007**, *32*, 109.
(10) Qin, Y.; Wang, X.; Wang, Z. L. *Nature* **2008**, *451*, 809.
(11) Choi, W. B.; Chu, J. U.; Jeong, K. S.; Bae, E. J.; Lee, J. W.; Kim, J. J.; Lee, J. O. *Appl. Phys. Lett.* **2001**, *79*, 3696.
(12) Tang, Y. B.; Cong, H. T.; Wang, Z. M.; Cheng, H. M. *Appl. Phys. Lett.* **2006**, *89*, 253112.
(13) Martinson, A. B. F.; Elam, J. W.; Hupp, J. T.; Pellin, M. J. *Nano Lett.* **2007**, *7*, 2183.
(14) Jiang, C. Y.; Sun, X. W.; Lo, G. Q.; Kwong, D. L.; Wang, J. X. *Appl. Phys. Lett.* **2007**, *90*, 263501.
(15) Greene, L. E.; Law, M.; Yuhas, B. D.; Yang, P. *J. Phys. Chem. B* **2007**, *111*, 18451.
(16) Mor, G. K.; Shankar, K.; Paulose, M.; Varghese, O. K.; Grimes, C. A. *Nano Lett.* **2006**, *6*, 215.
(17) Kannan, B.; Castelino, K.; Majumdar, A. *Nano Lett.* **2003**, *3*, 1729.
(18) Coakley, K. M.; McGehee, M. D. *Chem. Mater.* **2004**, *16*, 4533.
(19) Law, M.; Greene, L. E.; Johnson, J. C.; Saykally, R.; Yang, P. D. *Nat. Mater.* **2005**, *4*, 455.
(20) Zhu, K.; Neale, N. R.; Miedaner, A.; Frank, A. J. *Nano Lett.* **2007**, *7*, 69.
(21) Kopidakis, N.; Schiff, E.; Park, N. G.; van de Lagemaat, J.; Frank, A. J. *J. Phys. Chem. B* **2000**, *104*, 3930.
(22) Galoppini, E.; Rochford, J.; Chen, H.; Saraf, G.; Lu, Y.; Hagfeldt, A. Boschloo, N/A. *J. Phys. Chem. B* **2006**, *110*, 3930.
(23) Peng, K.; Xu, Y.; Wu, Y.; Yan, Y.; Lee, S. T.; Zhu, J. *Small* **2005**, *1*, 1062.
(24) Xi, J. Q.; Schubert, M. F.; Kim, J. K.; Schubert, E. F.; Chen, M.; Lin, S. Y.; Liu, W.; Smart, J. A. *Nat. Photonics* **2007**, *1*, 176.
(25) Hu, L.; Chen, G. *Nano Lett.* **2007**, *7*, 3249.
(26) Macak, J. M.; Tsuchiya, H.; Taveira, L.; Aldabergerova, S.; Schmuki, P. *Angew. Chem., Int. Ed.* **2005**, *44*, 7463.
(27) Funk, S.; Hokkanen, B.; Burghaus, U.; Ghicov, A.; Schmuki, P. *Nano Lett.* **2007**, *7*, 1091.
(28) Greene, L. E.; Law, M.; Tan, D. H.; Montano, M.; Goldberger, J.; Somorjai, G.; Yang, P. *Nano Lett.* **2005**, *5*, 1231.
(29) Tian, B.; Zheng, X.; Kempa, T. J.; Fang, Y.; Yu, N.; Yu, G.; Huang, J. *Nature* **2007**, *449*, 885.
(30) Nakamura, S. *Science* **1998**, *281*, 956.
(31) Ponce, F. A.; Bour, D. P. *Nature* **1997**, *386*, 251.
(32) Calarco, R.; Meijers, R. J.; Debnath, R. K.; Stoica, T.; Sutter, E.; Luth, H. *Nano Lett.* **2007**, *7*, 2248.
(33) Park, Y. S.; Park, C. M.; Fu, D. J.; Kang, T. W.; Oh, J. E. *Appl. Phys. Lett.* **2004**, *85*, 5718.
(34) Zhong, Z. H.; Qian, F.; Wang, D.; Lieber, C. M. *Nano Lett.* **2003**, *3*, 343.
(35) Kim, H. M.; Kim, D. S.; Park, Y. S.; Kim, D. Y.; Kang, T. W.; Chung, K. S. *Adv. Mater.* **2003**, *14*, 991.
(36) Yoo, J.; Hong, Y. J.; An, S. J.; Yi, G. C.; Chon, B.; Joo, T.; Kim, J. W.; Lee, J. S. *Appl. Phys. Lett.* **2006**, *89*, 043124.
(37) Deb, P.; Kim, H.; Rawat, V.; Oliver, M.; Kim, S.; Marshall, M.; Stach, E.; Sands, T. *Nano Lett.* **2005**, *5*, 1847.
(38) Hersee, H. D.; Sun, X.; Wang, X. *Nano Lett.* **2006**, *6*, 1808.
(39) Kuykendall, T.; Pauzauskie, P. J.; Zhang, Y. F.; Goldberger, J.; Sirbuly, D.; Denlinger, J.; Yang, P. D. *Nat. Mater.* **2004**, *3*, 524.
(40) Huang, Y.; Duan, X.; Cui, Y.; Lieber, C. M. *Nano Lett.* **2002**, *2*, 101.
(41) Qian, F.; Li, Y.; Gradecak, S.; Wang, D. L.; Barrelet, C. J.; Lieber, C. M. *Nano Lett.* **2004**, *4*, 1975.
(42) Qian, F.; Gradecak, S.; Li, Y.; Wen, C. Y.; Lieber, C. M. *Nano Lett.* **2005**, *5*, 2287.
(43) Johnson, J. C.; Choi, H. J.; Knutsen, K. P.; Schaller, R. D.; Yang, P. D.; Saykally, R. J. *Nat. Mater.* **2002**, *2*, 106.
(44) Kuykendall, T.; Pauzauskie, P.; Lee, S.; Zhang, Y.; Goldberger, J.; Yang, P. D. *Nano Lett.* **2003**, *3*, 1063.
(45) Choi, H. J.; Seong, H. K.; Chang, J.; Lee, K. I.; Park, Y. J.; Kim, J. J.; Lee, S. K.; He, R.; Kuykendall, T.; Yang, P. *Adv. Mater.* **2005**, *17*, 1351.
(46) Tang, Y. B.; Bo, X. H.; Lee, C. S.; Cong, H. T.; Chen, H. M.; Chen, Z. H.; Zhang, W. J.; Bello, I.; Lee, S. T. *Adv. Funct. Mater.*, in press.
(47) Yerokhov, V. Y.; Hezel, R.; Lipinski, M.; Clach, R.; Nagel, H.; Mylyanych, A.; Panek, P. *Sol. Energy Mater. Sol. Cells* **2002**, *72*, 291.
(48) Gangopadhyay, U.; Kim, K. H.; Mangalaraj, D.; Yi, J. S. *Appl. Surf. Sci.* **2004**, *230*, 364.
(49) Kanamori, Y.; Sasaki, M.; Hane, K. *Opt. Lett.* **1999**, *24*, 1422.
(50) Striemera, C. C.; Fauchet, P. M. *Appl. Phys. Lett.* **2002**, *81*, 2980.
(51) Beek, W. J. E.; Wienk, M. M.; Janssen, R. A. J. *Adv. Funct. Mater.* **2006**, *16*, 1112.

NL801728D